New pulse width modulation approach and model applied to multilevel inverters

Karima Berkoune, Paul-Etienne Vidal, Frédéric Rotella

NEW PULSE WIDTH MODULATION APPROACH AND MODEL APPLIED TO MULTILEVEL INVERTERS

K. BERKOUNE[1], P-E VIDAL[1], F.ROTELLA[1]

1. LGP, ENIT, Université of Toulouse, 47 Avenue d'Azereix BP 1629, 65016 Tarbes, France
e-mail : karima.berkoune@enit.fr

Abstract - This paper proposes a new approach to the Pulse Width Modulation strategies of multilevel Voltage Source Inverters. In this study, the modelling is focused on a flying capacitor three-level topology. This mathematical approach is based on the concepts of pseudo inverse and generalized inverse. The study allows recovering classical Pulse Width Modulation (PWM) solutions. It also offers a new investigative tool to explore the degree of freedom provided by the duty cycle solution set.

Keyword - Pulse Width Modulation, Voltage Source Inverters, Generalized Inverse, Optimisation, Multilevel Inverters.

1 INTRODUCTION

Static converters implementing schemes by Pulse Width Modulation (PWM), widely available in varaiable speed applicaiton such as railway applications, air planes but also in cars and both in industry with robots and in sevrices and home automation with uninterruptible power supplies. In addition, other applications using these technologies as renewable energy (solar and wind), and transportation with the Electric Vehicles opens new applications. All these application areas, with their constraints and performance criteria have led and still arouse a multitude of studies that develop, test and offer different converter structures or different conversion control algorithms. Multilevel inverters have received much attention in recent years. In several documents, many topologies have been introduced and extensively studied for utilities, traction, and application training [3]. These inverters are suitable for high voltage applications. They are also able to minimize the blocking voltage applied to semiconductors devices. In addition, the harmonic content of the output waveform significantly decreases when the number of levels increases [4], [5]. The multilevel inverters are generally classified as: clamped diode inverters, cascaded inverters and flying capacitor inverters. Among these categories, the three-level Neutral Point Clamped inverter (NPC) that belongs to diode clamped category has been widely used [6], [11]. However, it is difficult to control the real power flow for balancing the potential of the neutral point. Moreover, the extension to multiple levels is limited by the additional diodes. On the other hand, the flying capacitor inverter has a drawback in that it requires additional capacitors, and requires the balancing control of capacitor voltages [7], [1]. The Flying Capacitor topology (FC) is a series connection of switching cells as illustrated in Fig. 1. The major interest of flying capacitor converter [2] is to solve the problem of the voltage balance as well as to reduce the excessive number of diodes. It appears that the trend is to apply usual PWM issued from two-level inverters to multilevel structure as FC and NPC. Nevertheless another studies applied some more complex controls such as Space Vector Modulation (SVM) [3], [4]. The main objective of this study is to define a new approach of the carrier based PWM dedicated to multilevel inverter structure. Based on the use of generalized inverse theory, the duty cycle solution set is expressed for a three-level flying capacitor inverter. Finally, the study checks that some of the well-known PWM can be recovered by fixing some free parameters of this solution [12].

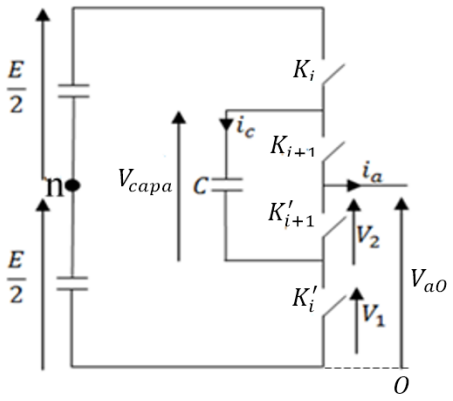

Fig. 1. One leg of three level flying capacitor inverter

2 THREE PHASE-THREE LEVEL FLYING CAPACITOR INVERTER

2.1 FLYING CAPACITOR MODEL

Figure 1 illustrates the one leg scheme of a three-level flying capacitor inverter. The switches are arranged in pairs within 2 commutation cells. The switches of a commutation cell should be in a complementary state such as

$$\begin{cases} c_i = \bar{c_i'} = 1 \Rightarrow K_i \quad \text{is ON, } K_i' \quad \text{is OFF,} \\ c_i = \bar{c_i'} = 0 \Rightarrow K_i \quad \text{is OFF, } K_i' \quad \text{is ON.} \end{cases} \tag{1}$$

Table 1 shows the possible switch states and the deduced leg voltage expression. It is noted that the leg voltage V_{lO} can reach three levels: $\{0, E/2, E\}$. We assumed that $V_{capa} = \dfrac{E}{2}$ in steady state.

I. Table of sequences

K_i	K_{i+1}	K_i'	$K_{i+1'}$	V_{lO}
1	1	0	0	E
1	0	0	1	$\dfrac{E}{2}$
0	1	1	0	$\dfrac{E}{2}$
0	0	1	1	0

For this study a three phase inverter is taken into account. Based on Fig. 1, it is composed of three identical legs.

$$V_{lO} \in \{V_{aO}, V_{bO}, V_{cO}\} \tag{2}$$

For each leg, it is obvious that

$$V_{aO} = V_1 + V_2 \tag{3}$$

Applying the average value over a switching period T_s, leads to

$$< V_1 >= \frac{E}{2}\alpha_{a1} \tag{4}$$

$$< V_2 >= \frac{E}{2}\alpha_{a2} \tag{5}$$

according to the leg number respectively, whereas α_{a1}, α_{a2} are the duty cycles of the two series commutation cell within the inverter leg. Finally the mean value of all legs voltage is obtained as

$$< V_{lO} >= \frac{E}{2}(\alpha_{l1} + \alpha_{l2}) \tag{6}$$

with $l \in \{a, b, c\}$. Each line voltage V_{lO} is expressed for each leg as a function of the duty cycles as,

$$\underline{V_{lO}} = \frac{E}{2}\begin{bmatrix} 1 & 1 & 0 & 0 & 0 & 0 \\ 0 & 0 & 1 & 1 & 0 & 0 \\ 0 & 0 & 0 & 0 & 1 & 1 \end{bmatrix} \underline{\alpha} \tag{7}$$

If the duty cycles are expressed as,

$$\underline{\alpha} = \begin{bmatrix} \alpha_{a1} & \alpha_{a2} & \alpha_{b1} & \alpha_{b2} & \alpha_{c1} & \alpha_{c2} \end{bmatrix}^T \tag{8}$$

For simplicity sake, we assume that the 3φ $R-L$ load is balanced, $Z = Z_1 = Z_2 = Z_3$ with Z the complex impedance, and star-connected to a neutral point, hereby noted N. We specify that N is different to n wihch is the DC-bus mid-point. It is deduced that:

$$V_{NO} = \frac{1}{3}\begin{bmatrix} 1 & 1 & 1 \end{bmatrix} \underline{V_{lO}} \tag{9}$$

$$\underline{V_{lN}} = \underline{V_{lO}} - \begin{bmatrix} 1 \\ 1 \\ 1 \end{bmatrix} V_{NO} \tag{10}$$

Consequently, the phase voltage is expressed as,

$$\underline{V_{lN}} = \frac{E}{6}\begin{bmatrix} 2 & 2 & -1 & -1 & -1 & -1 \\ -1 & -1 & 2 & 2 & -1 & -1 \\ -1 & -1 & -1 & -1 & 2 & 2 \end{bmatrix} \underline{\alpha} \tag{11}$$

with $\underline{V_{lN}} = [V_{aN} \quad V_{bN} \quad V_{cN}]^T$. Where the matrix F is expressed such as

$$\underline{V_{lN}} = \frac{E}{6} G \underline{\alpha} \tag{12}$$

It is noted that $rank(F) = 2$. It is obviously due to the fact that

$$V_{aN} + V_{bN} + V_{cN} = 0, \tag{13}$$

Consequently, expression (11) is reduced to

$$\begin{aligned} \underline{V_{lN}} &= \frac{E}{6}\begin{bmatrix} 2 & 2 & -1 & -1 & -1 & -1 \\ -1 & -1 & 2 & 2 & -1 & -1 \end{bmatrix} \underline{\alpha} \\ &= \frac{E}{6} F \underline{\alpha} \end{aligned}, \tag{14}$$

with $\underline{V_{lN}} = [V_{aN} \quad V_{bN}]^T$. Due to singularity of the F matrix, we cannot obtain the reference duty cycle by applying the usual inverse. Effectively, it does not exist. The purpose of the next section is to overcome this drawback.

2.2 GENERALIZED INVERSE THEORY

It is well known that each square and non-singular matrix A has a unique inverse, named A^{-1}, which satisfies

$$AA^{-1}A = A \tag{15}$$

For every matrix, a generalized inverse, $A_{[1]}$, is defined such as

$$AA^{[1]}A = A \tag{16}$$

The pseudo-inverse of each matrix A, noted $A^{\dagger}$ is defined. As the generalized inverse is not unique, we are

looking for specific matrices satisfying the four Penrose properties.

$$\begin{cases} AA^{\dagger}A = A \\ A^{\dagger}AA^{\dagger} = A^{\dagger} \\ (AA^{\dagger})^{*} = A^{\dagger}A \\ (A^{\dagger}A)^{*} = AA^{\dagger} \end{cases} \tag{17}$$

It is obvious that $A^{\dagger}$ is a particular generalized inverse of A. The purpose of the theory of generalized inverse is to get the set of linear systems [14] of the solution. Let us consider a linear system described by:

$$AX = Y \tag{18}$$

Using the notion of generalized inverse, all the solution is expressed by:

$$X = A^{\dagger}Y + (I_m - A^{\dagger}A)z \tag{19}$$

where Z is an arbitrary matrix. $A^{\dagger}$ can easily be calculated numerically.

2.3 New degrees of freedom

Thanks (19), the solution set for leg duty cycles is obtained by

$$\underline{\alpha} = F^{\dagger}\underline{V_{ref}} + (I_6 - F^{\dagger}F)\underline{z} \tag{20}$$

where $F^{\dagger}$ is the pseudo inverse of F obtained in (14), and I_6 is the identity matrix. $F^{\dagger}$ is obtained thanks to numeric computation by using matrix calculus software, for instance Scilab [15]. Duo to the pseudo inverse process, the desired leg reference voltages are now inserted in $\underline{V_{ref}}$.Finally, the duty cycles for each leg and commutation cells are expressed:

$$\begin{aligned} \underline{\alpha} \quad = & \frac{1}{E}\begin{bmatrix} 1 & 0 \\ 1 & 0 \\ 0 & 1 \\ 0 & 1 \\ -1 & -1 \\ -1 & -1 \end{bmatrix} \begin{bmatrix} V_{ref_{aN}} \\ V_{ref_{bN}} \end{bmatrix} \\ & + \frac{1}{3}\begin{bmatrix} 2 & -1 & 1/2 & 1/2 & 1/2 & 1/2 \\ -1 & 2 & 1/2 & 1/2 & 1/2 & 1/2 \\ 1/2 & 1/2 & 2 & -1 & 1/2 & 1/2 \\ 1/2 & 1/2 & -1 & 2 & 1/2 & 1/2 \\ 1/2 & 1/2 & 1/2 & 1/2 & 2 & -1 \\ 1/2 & 1/2 & 1/2 & 1/2 & -1 & 2 \end{bmatrix} \begin{bmatrix} z_1 \\ z_2 \\ z_3 \\ z_4 \\ z_5 \\ z_6 \end{bmatrix} \end{aligned} \tag{21}$$

It is noted that $rank(I_6 - F^{+}F) = 4$. Consequently 4 Degrees Of Freedom (DOF) are defined:

$$\underline{\lambda} = \begin{bmatrix} \lambda_1 & \lambda_2 & \lambda_3 & \lambda_4 \end{bmatrix}^T \tag{22}$$

Whith such definition, the aim is to reduce the size of thefree component of (21). This is the reason why, the rank factorization of $rank(I_6 - F^{+}F)$ is given as

$$\begin{aligned} & (I_6 - F^{+}F) = \\ & \frac{1}{3}\begin{bmatrix} -1 & 0 & 0 & 1 \\ 1 & 0 & 0 & 1 \\ 0 & -1 & 0 & 1 \\ 0 & 1 & 0 & 1 \\ 0 & 0 & -1 & 1 \\ 0 & 0 & 1 & 1 \end{bmatrix} \cdot \\ & \begin{bmatrix} -3/2 & 3/2 & 0 & 0 & 0 & 0 \\ 0 & 0 & -3/2 & 3/2 & 0 & 0 \\ 0 & 0 & 0 & 0 & -3/2 & 3/2 \\ 1/2 & 1/2 & 1/2 & 1/2 & 1/2 & 1/2 \end{bmatrix} \end{aligned} \tag{23}$$

Indeed, DOF are expressed as

$$\underline{\lambda} = \begin{bmatrix} -3/2 & 3/2 & 0 & 0 & 0 & 0 \\ 0 & 0 & -3/2 & 3/2 & 0 & 0 \\ 0 & 0 & 0 & 0 & -3/2 & 3/2 \\ 1/2 & 1/2 & 1/2 & 1/2 & 1/2 & 1/2 \end{bmatrix} \underline{z} \tag{24}$$

Finally the duty cycle solution set is given

$$\begin{aligned} \underline{\alpha} = & \frac{1}{E}\begin{bmatrix} 1 & 0 \\ 1 & 0 \\ 0 & 1 \\ 0 & 1 \\ -1 & -1 \\ -1 & -1 \end{bmatrix} \begin{bmatrix} V_{ref_{aN}} \\ V_{ref_{bN}} \end{bmatrix} \\ & + \frac{1}{3}\begin{bmatrix} -1 & 0 & 0 & 1 \\ 1 & 0 & 0 & 1 \\ 0 & -1 & 0 & 1 \\ 0 & 1 & 0 & 1 \\ 0 & 0 & -1 & 1 \\ 0 & 0 & 1 & 1 \end{bmatrix} \begin{bmatrix} \lambda_1 \\ \lambda_2 \\ \lambda_3 \\ \lambda_4 \end{bmatrix} \end{aligned} \tag{25}$$

It is noted that each arm gets its own degree of freedom $\{\lambda_1, \lambda_2, \lambda_3\}$ whereas λ_4 is common to all legs.

3 Simulation results

The purpose of this section is to recover some various original and usual PWM solutions by using new DOF expressed, given in (25). The inverter structure applied is a three-pahse voltage inverter. The three line voltages are connected with $R = 15\,\Omega$ and $L = 1\,mH$ balanced three phases load. Indeed four case studies have been carried out. For each the following reference voltages are considered:

$$V_{ref}(t) = \begin{cases} V_{max}\cos(\omega t) \\ V_{max}\cos(\omega t - \frac{2\pi}{3}) \\ V_{max}\cos(\omega t - \frac{4\pi}{3}) \end{cases} \tag{26}$$

In this study the values are set to $V_{max} = \frac{E}{4}$ whereas ω=315. Indeed a linearity voltage zone functioning is guaranteed. At the beginning, the well known PWM

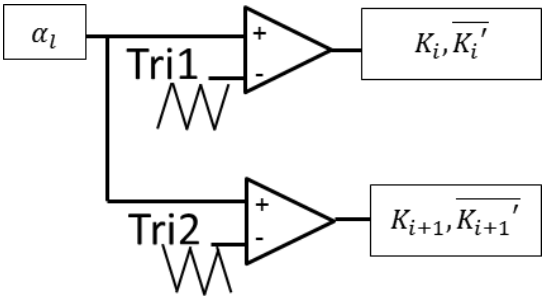

Fig. 2. Usual PWM scheme

scheme is applied, as illustrated in Fig. 2. The both triangle signals are included within [0;1]. They are out of phase of 180°. Their frequency is set to the switching frequency such as $T_s = 2000\,Hz$. The following three case consists in setting the DOF in order to be able to recover usual duty cyles applied. As far as the last study is concerned, the fourth case study, a new PWM scheme is applied.

3.1 First case

According to expression (25) the duty cycle used in the conventional case, is recovered with

$$\begin{aligned} &\lambda_1 = \lambda_2 = \lambda_3 = 0 \\ &\lambda_4 = 0 \end{aligned} \tag{27}$$

In such a case, the physical link between the duty cycle and the waveforms α is not satisfied. Effectively each duty cycle α_l is included within $[-1/2; 1/2]$, such as

$$-\frac{1}{2} \leq \alpha_l \leq \frac{1}{2} \tag{28}$$

Accordingly, the carriers must also evolve between $-\frac{1}{2}$ and $\frac{1}{2}$.

3.2 Second case

In order to improve the accuracy of our model, λ_4 is tuned to

$$\lambda_4 = \frac{3}{2} \tag{29}$$

Nevertheless $\{\lambda_1, \lambda_2, \lambda_3\}$ are still null. Consequently the duty cyle applied are

$$\underline{\alpha} = \frac{V_{ref}}{E} + \frac{1}{2}\underline{U} \tag{30}$$

With $\underline{U} = [1 \quad 1 \quad 1]^T$. Consequently, new boundaries are expressed as

$$0 \leq \alpha_l \leq 1 \tag{31}$$

The Figure 3 illustrates the waveforms of the two duty cycle applied per leg.

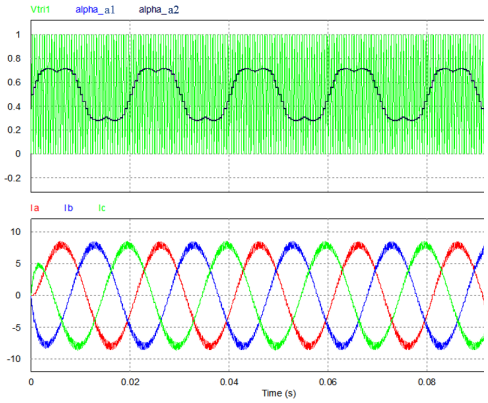

Fig. 3. Waveforms obtained for the most simple case

The leg voltage is also monitored as well as the three line currents. The choice of DOF is checked for the classical case. Nevertheless a better use of the DOF can be expected.

3.3 Third case

In this case a zero sequence signal is added to the duty cycle by the mean of λ_4. $\{\lambda_1, \lambda_2, \lambda_3\}$ are set to 0 such as

$$\begin{aligned} &\lambda_1 = \lambda_2 = \lambda_3 = 0 \\ &\lambda_4 = \tfrac{3}{2} + \mu \end{aligned} \tag{32}$$

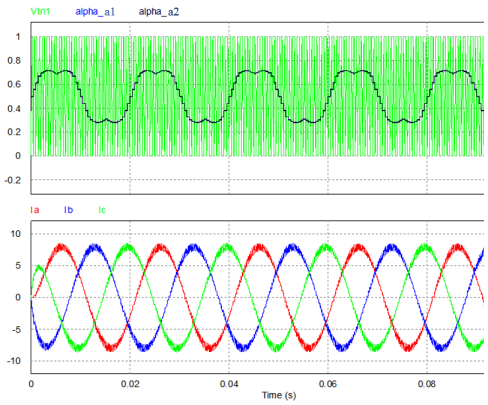

Fig. 4. New duty cycle and currents for zero sequence signal

In order to tune μ, we compute expression (10) with (25), taking into account the average value. Thanks to each phase voltage, λ_4 is deduced by fixing

$$\mu = \frac{3V_{NO}}{E} \tag{33}$$

By this mean the boundaries are still defined similarly as stated in Eq. (31). Finally the duty cycle is ex-

pressed as

$$\underline{\alpha} = \frac{V_{ref}}{E} + \frac{1}{2}\underline{U} + \frac{V_{NO}}{E}\underline{U} \tag{34}$$

In such duty cycles, the most common case encountered is realised where

$$V_{NO} = \frac{V_{med}}{2} \tag{35}$$

V_{med} is the medium value of the load voltage $\underline{V_{lN}}$. It is expressed as:

$$\frac{V_{med}}{2} = -\frac{max(V_{ref}) + min(V_{ref})}{2} \tag{36}$$

The simulation results are illustrated in Fig. 4. Moreover this solution extend the voltage linearity zone. The given boundaries for μ are similar to those shown in a common three phase inverter, [10]. In the first three cases, the duty cycle within an arm are identical, allowing a pattern of the Fig. 2.

3.4 Fourth case

The third previous cases allow recovering simply the usual PWM applied to multilevel inverters. Nevertheless, it is noted that self leg DOF, $\{\lambda_1, \lambda_2, \lambda_3\}$ respectively, are not used.

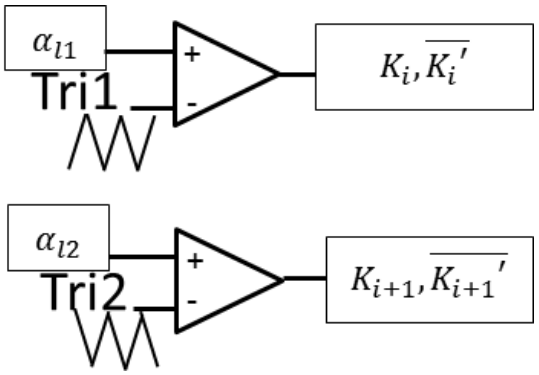

Fig. 5. New PWM scheme

In order to check the possibility of using them, a new PWM scheme is applied, as illustrated in Fig. 5. In such a manner the DOF $\{\lambda_1, \lambda_2, \lambda_3\}$ can directly interact on the leg duty cycle. These DOF are set to an arbitrary sine waveform, such as

$$\begin{aligned} \lambda_1 &= \tfrac{V_{max}}{6E} sin(3wt) \\ \lambda_2 &= \tfrac{V_{max}}{6E} sin(3wt - \tfrac{2\pi}{3}) \\ \lambda_3 &= \tfrac{V_{max}}{6E} sin(3wt - \tfrac{4\pi}{3}) \\ \lambda_4 &= \tfrac{3}{2} + \mu = \tfrac{3}{2} + \tfrac{3V_{NO}}{E} \end{aligned} \tag{37}$$

It is represented by Fig. 6.

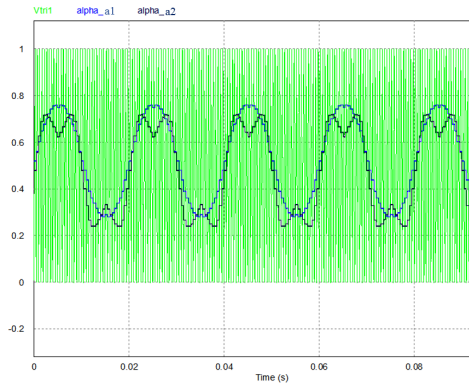

Fig. 6. New duty cycle obtained for the first leg when λ_1 is set to a sine waveform

For each leg the overall duty cycle is similar to (34) because:

$$\alpha_l = \frac{\alpha_{l1} + \alpha_{l2}}{2} \tag{38}$$

Thanks to dispatching, it is possible to adjust λ_1 and λ_2 differently without jeopardizing the overall strategy (which connects the arm tension with the duty cycle). It is noted that each DOF can be adjust in order to match some criteria to be defined. In the above example, it is noted that the waveforms are not affected by this choice. It is checked that the currents does not suffer from that choice. Indeed, the voltage Fourier transform witch are illustrated in Fig. 7 and Fig. 8 respectively, are ploted for both case:

$$\lambda_1 = \begin{cases} 0 & \text{in Fig. 7} \\ \frac{V_{max}}{6E} sin3wt & \text{in Fig. 8} \end{cases} \tag{39}$$

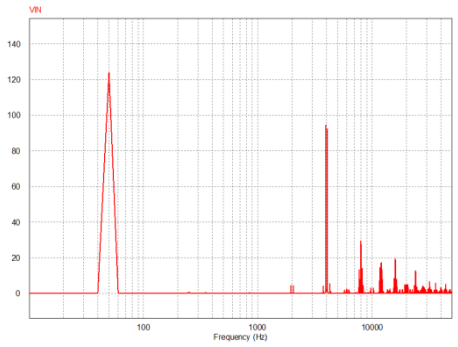

Fig. 7. FFT of a phase leg voltage with a null $\lambda_1, \lambda_2, \lambda_3$

The biggest influence of the sine appearance is highlighted by green circle, Fig. 8. As said previously this DOF acts direclty on the duty cycle dispatching within an inverter leg. So it is interesting to monitor

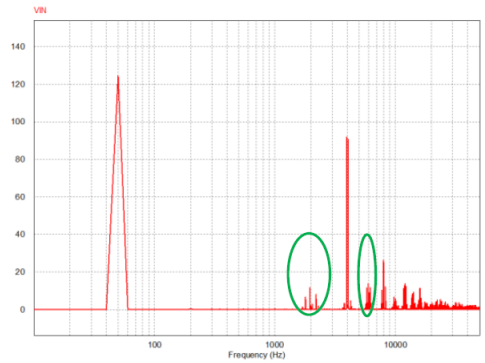

Fig. 8. FFT of a phase leg voltage with a sine $\lambda_1, \lambda_2, \lambda_3$

the capacitor voltage. In the following Fig. 8 and Fig. 9 the capacitor voltages are displayed, where V_{capa} is the voltage across the capacitor. It appears that using

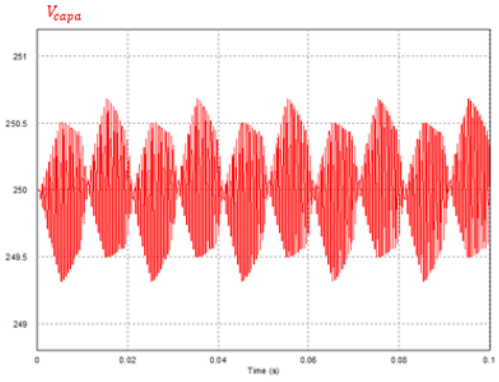

Fig. 9. Capacitor voltage with a null $\lambda_1, \lambda_2, \lambda_3$

$\{\lambda_1, \lambda_2, \lambda_3\} \neq 0$ has a direct incidence on the capacitor voltage. The next stage in that work is to be able to link the values$\{\lambda_1, \lambda_2, \lambda_3\}$ to defined criteria as done for λ_4.

4 Conclusion

This paper deals with a new mathematical approach for carrier based Pulse Width Modulation schemes, applied to multilevel inverter modelling. An average mode is used combined with the generalized inverse theory in order to reveal the maximum degrees of freedom allowed in such a structure. The usual PWM applied are retrieved. It is also demonstrated that it exists for each inverter leg a specific degree of freedom. It can be fixed in order to improve some criteria that have to be defined. Some simulation results are provided.

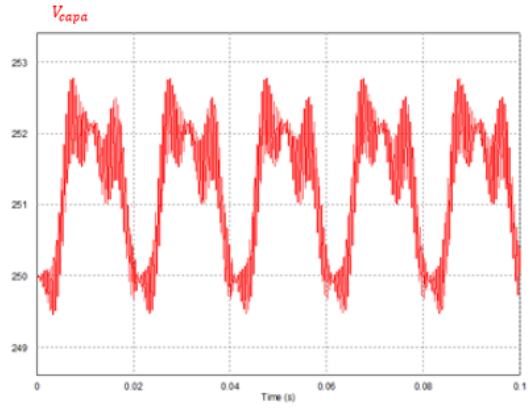

Fig. 10. Capacitor voltage with a sine $\lambda_1, \lambda_2, \lambda_3$

References

[1] A. K. Rathor, J. Holtz and T. Boller, Synchronous optimal Pulse Width Modulation for Low-Switching-Frequency Control of Medium-Voltage Multilevel inverter, IEEE Transactions on Industrial Electronics, vol.57 n°7, July 2010, pp.2374-2381.

[2] P. C. Loh, D. G. Holmesand and T. A. Lipo, Implementation and control of distributed PWM cascaded multilevel inverters with minimal harmonic distortion and common mode voltage, Power Electronics, IEEE Transactions on, vol.20, Issue:1, January 2005, pp.90-99.

[3] C. Hochgraf, R.Lasseter, D. Divan and T.Lipo, Comparaison of multilevel inverters for static var compensation, IEEE-IAS Annual Meeting, vol.2, 1994, pp.921-928.

[4] T. A. Meynard and H. Foch, Multilevel Conversion: High voltage choppers and voltage source inverter, IEEE PESC 92, vol.1,1992, pp.397-403.

[5] J. Rodriguez, J-S Lai and FZ Peng, Multilevel Inverter: A survey of topologies, controls and applications, IEEE Transaction on Industrial electronics, vol 49, n°4, pp.724-738, August 2002.

[6] A. Nabae, I. Takahashi and H. Akagi, A new neutral-point-clamped PWM inverter, IEEE Transactions on Industrial Application, vol.17, n°5, PP.518-523, Sep/oct 1981.

[7] M. Gasulla-Fomer, J. Jordana-Barnils, R. Pallas-Areny and J.M. Torrents, The floating capacitor as a differential building block, IEEE Transactions on instrumentation and Measurement, vol.47, n°.1,pp.26-29, February 1998.

[8] C. Newton and M. Summer, Multilevel inverter a real solution to medium/high-voltage drives, Power Eng.J, vol.12, n°1, pp.21-26, February 1998.

[9] D. Youssouf and B. A. Djamal, Modélisation et commande d?un onduleur triphasé piloté par MLI a structure multiniveaux, Diplôme de master en Génie Electrique, 2012.

[10] P. E. Vidal, S. Cailhol, F. Rotella, K. Berkoune, A. Llor and M. Fadel, Generalized inverse applied to Pulse Width Modulation for static conversion, Power Electronic and application EPE, European conference on, pages 1-10, Lille, September 2013.

[11] M. Veenstra, Investigation of hybrid asymmetric multi-level inverter for medium voltage applications, School polytechnic Federal of Lausanne, 2003.

[12] McGrath, T. Meynard, G. Gateau, D.G. Holmes, Optimal Modulation of Flying Capacitor and Stacked Multicell Converters Using a State Machine Decoder, Power Electronics, IEEE Transactions on (Volume:22 , Issue: 2), March 2007, Page(s):508-516.

[13] S. J. Watkins, Sch. of Electron. & Electr. Eng., Leeds Univ., UK ; Zhang, L.Multilevel space vector PWM control schemes for a flying-capacitor inverter, Power Electronics, Machines and Drives, 2004. (PEMD 2004). (Volume:1)31 March-2 April 2004, Page(s):12-17.

[14] V. Lovass-Nagy, R. J. Miller, and D. L. Powers, An introduction to the application of the simplest matrix-generalized inverse in systems science, Proc. IEEE Trans. Circuits and Systems, vol CAS-25, pp. 766-771, 1978.

[15] Scilab: Le logiciel open source gratuit de calcul numerique, Scilab Enterprises, Orsay, France, 2012, http://www.scilab.org